

**Attosecond-pulse production using resonantly enhanced high-order harmonics**

V. V. Strelkov\*

*A. M. Prokhorov General Physics Institute of the RAS, Moscow 119991, Russia  
and Moscow Institute of Physics and Technology (State University), 141700 Dolgoprudny, Moscow Region, Russia*  
(Received 26 October 2016; published 23 December 2016)

We study theoretically the effect of giant resonance in Xe on the phase difference between consecutive resonantly enhanced high-order harmonics and calculate the duration of the attosecond pulses produced by these harmonics. For certain conditions, resonantly induced dephasing compensates the phase difference which is intrinsic for off-resonance harmonics. We find these conditions analytically and compare them with numerical results. This harmonic synchronization allows attosecond-pulse shortening in conjunction with the resonance-induced intensity increase of more than an order of magnitude. The latter enhancement relaxes the requirements for the UV filtering needed for attosecond-pulse production. Using a two-color driving field allows a further increase of the intensity. In particular, a causticlike feature in the harmonic spectrum leads to a generation efficiency growth of up to two orders of magnitude, which is, however, accompanied by an elongation of the XUV pulse.

DOI: 10.1103/PhysRevA.94.063420

**I. INTRODUCTION**

Attosecond-pulse production using high-order harmonics generated by an intense laser field [1,2] is essentially based on the phase locking of the harmonics. This phase locking is well understood [3,4] for the case when there are no resonances affecting the process. However, recently much attention has been paid to the role of resonances in high-harmonic generation (HHG) in gases [5–8] and plasma plumes [9–11] (for a review of earlier studies, see also Refs. [12,13]). It was shown that when the high-harmonic frequency is close to the transition to an excited quasistable state of the generating particle, the harmonic can be much more intense than the off-resonant ones. For the HHG in plasma plumes such an enhancement can be as high as an order of magnitude greater. An enhancement of the efficiency of XUV generation due to giant resonance in Xe was predicted in Ref. [14] and observed in Refs. [6,7]. Namely, the XUV near 100 eV in the spectral region of about 20 eV is more intense than the lower-frequency XUV, and the enhancement near the center of the resonance is approximately an order of magnitude.

Broadband resonant enhancement potentially allows generating attosecond pulses using resonant harmonics. This approach is interesting not only because of the higher generation efficiency of the resonant HH, but also because it essentially reduces the requirements for harmonic filtering (the resonant region naturally stands out). However, phase locking of resonant HH differs from the one of nonresonant HH [10], so attosecond-pulse production in the former case is not straightforward. In this paper we investigate this aspect of resonant HHG both numerically and analytically. We study the effect of resonance on the phase difference between the neighboring harmonics and calculate the duration of the attosecond pulses produced by resonant harmonics.

**II. HARMONIC PHASE NEAR THE RESONANCE; “RESONANT ATTOCHIRP”**

The time-dependent three-dimensional Schrödinger equation (TDSE) is solved numerically for a single-active electron

atom in an external laser field. The method of the numerical TDSE solution is described in Ref. [15]. The model atomic potential is (atomic units are used throughout)

$$V(r) = -a_0 \exp\left(-\frac{r^2}{b_0^2}\right) + a_1 \exp\left(-\frac{(r-r_0)^2}{b_1^2}\right). \quad (1)$$

The first term is the binding potential of the atomic core, and the second one is the barrier providing a quasistable state with positive energy (such states are also denoted as the “resonance states”). The potential is similar to the one used earlier in resonant HHG calculations [16–18]. Moreover, a double-barrier effective potential was found in Ref. [19] describing autoionization in time-dependent density-functional theory.

In the potentials that we used in Refs. [16,18] the first term is a soft-Coulomb potential, whereas in the potential (1) it is Gaussian. Such a potential does not have Coulomb “tails” and thus does not support Rydberg states; however, it provides more freedom to simulate the properties of the desired atom. Choosing the parameters  $a_0$ ,  $a_1$ ,  $b_0$ ,  $b_1$ , and  $r_0$  of the model potential, we reproduce the ionization energy of the Xe atom, and the frequency and width of the giant resonance so that the frequency and width of the resonantly enhanced region in the calculated HH spectrum is close to those observed in Ref. [6]. The parameters of the potential used in our calculations are  $a_0 = 7.1$ ,  $b_0 = 1.0$ ,  $a_1 = 4.5$ ,  $b_1 = 0.5$ , and  $r_0 = 1.23$  a.u. Throughout this paper we simulate only the shortest electronic trajectory (if not specifically stated otherwise), suppressing the others with a properly defined absorbing region in the numerical box, as it was done in Ref. [20].

The laser field intensity is switched on smoothly during four optical cycles, then it is constant during four cycles, and then it decreases during four cycles; the shape of the laser pulse is described in Ref. [21]. We are using either a single-color driving field or a two-color one. The two-color field is given by

$$E(t) = E_0 f(t) [\exp(-i\omega_l t) + \sqrt{\alpha} \exp(-i2\omega_l t + i\phi)] + \text{c.c.}, \quad (2)$$

where  $E_0$  is the amplitude of the main component of the laser field,  $\omega_l$  is its frequency,  $f(t)$  is the slowly varying envelope,

\*strelkov.v@gmail.com

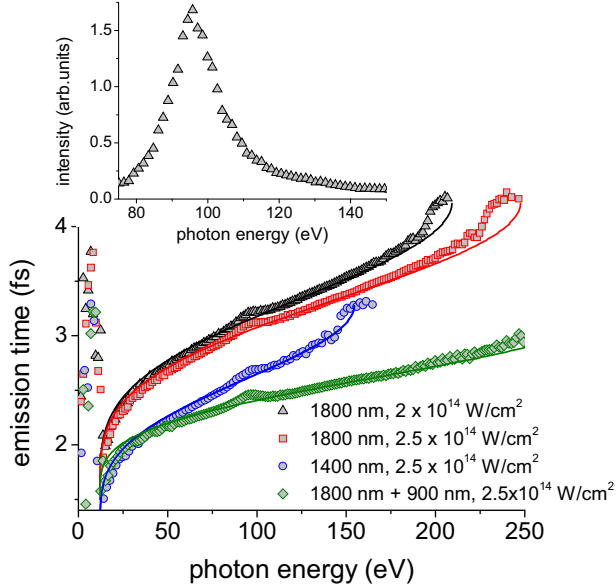


FIG. 1. Emission time calculated via numerical TDSE solution (symbols) and the estimates of this time as a classical return time of the electron in the simple-man model (solid lines). The driving laser intensities and wavelengths are shown in the graph; the two-color field is given by Eq. (2) with  $\alpha = 1$  and  $\phi = \pi/2$ . The inset shows harmonic intensities near the resonance.

$\alpha$  is the ratio of the intensities of the driving field components, and  $\phi$  is the relative phase.

We calculate the harmonic spectrum and find the spectral phase differences between the consecutive harmonics. Then we calculate the emission times  $t_e(q\omega_l) = (\varphi_{q+1} - \varphi_{q-1})/(2\omega_l)$ , where  $q$  is an even number, and  $\varphi_{q\pm 1}$  are the harmonic spectral phases;  $t_e$  characterizes the time instant when an attosecond pulse formed by a group of harmonics with the central frequency  $q\omega_l$  is emitted [22]. The results are shown in Fig. 1 for different laser intensities and wavelengths together with the classical electronic return times  $t_r(q\omega_l)$  calculated within the simple-man's approach [23,24]. Times  $t_e$  and  $t_r$  in general are close to each other [3]; the agreement is very good under the conditions of our calculations, which are well within the tunneling regime of ionization. However, the pronounced deviation from the classical prediction can be seen in the cutoff region and in the resonant region. The phase locking of the harmonics near the cutoff was studied recently in detail in Ref. [25]; in this paper we will study the harmonic phase locking in the resonant region.

The inset in Fig. 1 shows the harmonic spectrum near the resonance. The group of harmonics centered at approximately 96 eV is enhanced, and the generation efficiency in the center of the resonance is about an order of magnitude higher than it is far from it. The width of the resonantly enhanced harmonic group is 17 eV [full width at half maximum (FWHM)].

Figure 2 shows the emission times for these harmonics. To calculate these emission times we used harmonic phases averaged over ten laser intensities in the vicinity (within  $\pm 2\%$ ) of the intensity presented in the figure; this is done to reduce the numerical noise. We can see that the emission time is affected by the resonance: The resonant harmonics

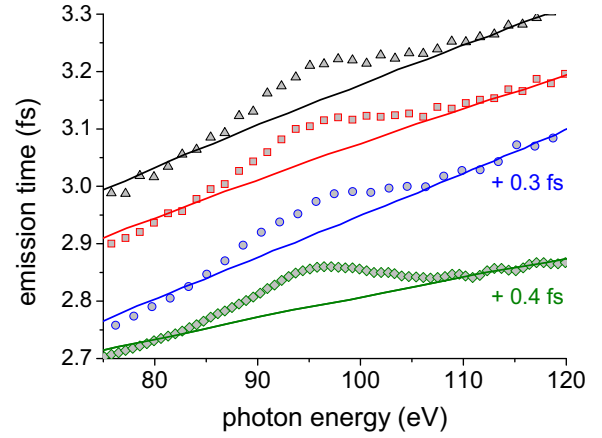


FIG. 2. Closeup of the harmonic emission times near the resonance. The fields' parameters are the same as in Fig. 1.

are emitted *later* than they would be emitted in the absence of resonance. This result is in agreement with the published experimental results for HHG in  $\text{Sn}^+$  [10], as well as analytical and numerical studies [17,18]. The delay time found for the harmonics near the center of the resonant line (68 as) is close to the lifetime of the quasistable state (77 as). This result can be well understood within the four-step model of the resonant HHG [16]: The resonant XUV emission is delayed with respect to the nonresonant one, and the delay time is the time which the system stays in the quasistable state after rescattering.

The resonant-induced delay of the XUV emission smoothly decreases with an increase of the detuning from the resonance. So, in the spectral region above the resonance this “resonant attochirp” can compensate the usual “free-motion attochirp” (the one caused by the free electronic motion before rescattering). Let us estimate both these chirps and their influence on the attosecond-pulse duration.

To do this we consider the chirped Gaussian attopulse,

$$F(t) = \exp(-i\Omega t) \int_{-\infty}^{+\infty} \exp \left[ -2 \ln(2) \left( \frac{\omega'}{\Delta\omega} \right)^2 \right] \times \exp \left( i \frac{K}{2} \omega'^2 \right) \exp \{ -i\omega' [t - t_r(\Omega)] \} d\omega', \quad (3)$$

where  $\Omega$  is the central frequency of the pulse and  $t_r(\Omega)$  is the emission time of the pulse. Let us assume that the chirp of the pulse is only due to the variation of the emission frequency described by the simple-man's model (below we denote this chirp as the “free-motion-induced attochirp”). Thus the derivative of the spectral phase [ $\varphi \equiv \frac{K}{2} \omega'^2 + t_r(\Omega) \omega'$ ] over the frequency  $\omega'$  is the classical electronic return time  $t_r(\omega')$ . So,  $K = \partial t_r / \partial \omega'$ . From Fig. 1 we can see that  $t_r$  is an almost linear function of  $\omega'$  except for the lowest and the highest parts of the plateau. This linear approximation can be found from the solution of the Newton's equation for the electron in the simple-man model. We find that approximately

$$K = 1/(2\omega_l U_p), \quad (4)$$

where  $U_p$  is the ponderomotive energy. The duration of the chirped pulse (3) depends on its spectral width  $\Delta\omega$ . The shortest duration is achieved when  $\Delta\omega = \sqrt{4 \ln(2)/K}$ .

Substituting (4) in the latter equation, we find that

$$\Delta\omega = 2\sqrt{2\ln(2)U_p\omega_l}. \quad (5)$$

The duration (FWHM of intensity) of this pulse is

$$\tau = 2\sqrt{\ln(2)/(U_p\omega_l)}. \quad (6)$$

Estimates (5) and (6) agree very well with the numerical TDSE calculations for the off-resonant harmonics. A similar estimate of the shortest attosecond-pulse duration was found in Ref. [26]. Note that Eq. (6) shows that  $\tau \propto \sqrt{\omega_l/I}$ , where  $I$  is the laser intensity. Since the maximum laser intensity is practically limited by the target ionization, this equation shows that the minimum attopulse duration decreases with a decrease in the laser frequency.

The ‘‘resonantly induced attochirp’’ can be estimated taking into account the delay in the resonant XUV emission. As we discussed above, this delay is the lifetime of the resonance (denoted below as  $\Delta t$ ) for the XUV in the center of the resonance, and it vanishes within the width of the resonance  $\Gamma$ . So, the resonantly induced attochirp is  $K_{\text{res}} = -\Delta t/\Gamma$ . Having in mind that  $\Delta t = 1/\Gamma$ , we find that  $K_{\text{res}} = -\Gamma^{-2}$ . From this equation and Eq. (4) we find that  $K = -K_{\text{res}}$  for

$$\Gamma = \sqrt{2U_p\omega_l}. \quad (7)$$

The conditions of our calculations for the single-color driving field were chosen so that the latter equation is approximately satisfied: We can see that in Fig. 2 the free-motion-induced attochirp is compensated with the resonantly induced one, so the group of harmonics above the central frequency of the resonance has approximately the same phases. In contrast to this, the parameters of the two-color field used in our calculations lead to a smaller free-motion-induced attochirp, so the resonantly induced one dominates.

### III. DURATION OF RESONANTLY ENHANCED ATTOSECOND PULSES

In Figs. 3 and 4 we show the attosecond pulses calculated using XUV from different spectral regions. Namely, using the complex amplitudes of the microscopic response  $d(\omega)$  calculated via the numerical TDSE solution, we find the XUV intensity,

$$I(t) = \left| \int_{\omega=-\infty}^{\infty} M(\omega)d(\omega)\exp(-i\omega t)d\omega \right|^2, \quad (8)$$

where the used spectrum mask  $M(\omega)$  is either a Gaussian,  $M_G(\omega) = \exp\{-2\ln(2)[(\omega - \Omega)/\Delta\omega]^2\}$ , or a steplike function,  $M_{\text{step}}(\omega) = \theta(\omega - \omega_{\text{low}})\theta(\omega_{\text{high}} - \omega)$ . In Fig. 3 we present the attopulses formed by resonant harmonics below the resonance (calculated using  $M_{\text{step}}$  with  $\omega_{\text{low}} = 60$  eV and  $\omega_{\text{high}} = 96$  eV), above it ( $\omega_{\text{low}} = 96$  eV and  $\omega_{\text{high}} = 130$  eV), and all the resonant harmonics ( $\omega_{\text{low}} = 60$  eV and  $\omega_{\text{high}} = 130$  eV). We can see that the attosecond pulse formed by the harmonics above the resonance is much shorter than the one formed by those below the resonance. This is because the above-resonant harmonics are in phase, whereas those below the resonance have significant phase differences (see Fig. 2), as it was discussed above. In the same figure we show the attopulse formed by the off-resonance harmonics calculated using  $M_G$  with a central frequency  $\Omega = 155$  eV and width

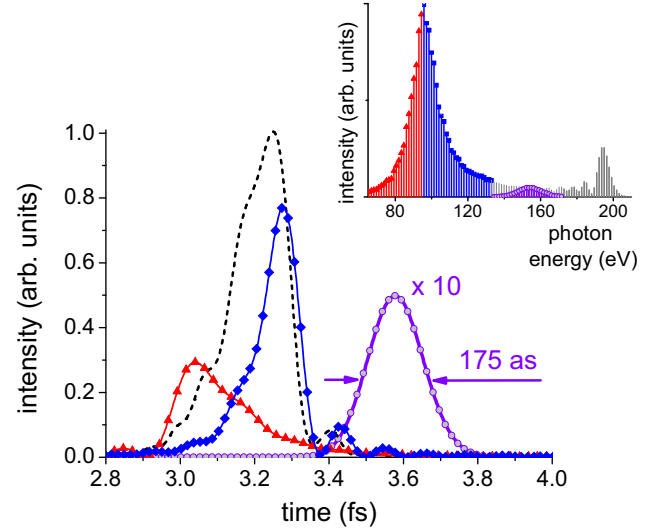


FIG. 3. Attosecond pulses calculated via Eq. (8) using resonantly enhanced harmonics below the center of the resonance (red lines with triangles), above the center of the resonance (blue lines with diamonds), all resonantly enhanced harmonics (dashed black line), and the group of off-resonant harmonics chosen to minimize the attopulse duration (violet line with circles); the latter attopulse is multiplied by 10 (see text for more details). The inset shows the harmonic spectrum; the spectral regions used to calculate the attosecond pulses are highlighted with the corresponding colors. The laser wavelength is 1800 nm and the intensity is  $2 \times 10^{14}$  W/cm<sup>2</sup>.

$\Delta\omega = 15.2$  eV. The latter is found numerically to minimize the pulse duration; the found width and duration are very close to the predictions of Eqs. (5) and (6), respectively. We can see that this pulse is slightly longer and much weaker than the one formed by the above-resonance harmonics. Moreover, if all the resonant harmonics are used to produce the attopulse, its duration does not increase dramatically (see the dashed line in Fig. 3).

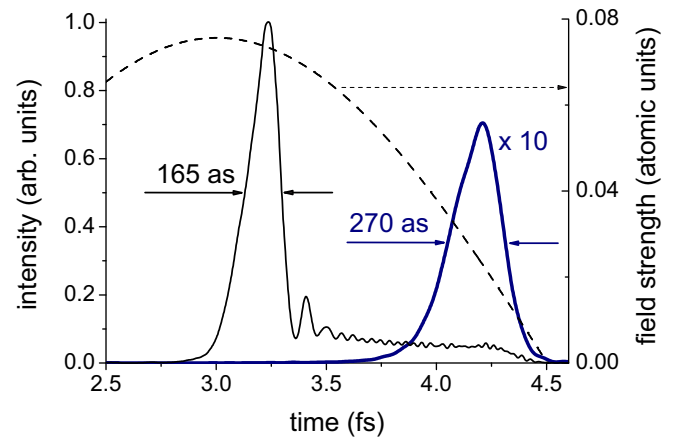


FIG. 4. Attosecond pulses formed by all harmonics higher than 60 eV (thin black line) and higher than 190 eV (thick navy line); the latter is multiplied by 10. The instantaneous strength of the laser field is shown with a dashed line. The laser parameters are the same as in Fig. 3.

Metal foils or multilayer mirrors are usually applied as spectral filters [1,2,27,28] to obtain attosecond pulses; such filters, in particular, can transmit well all UV higher than a certain frequency. To simulate the attosecond pulses obtained with such a filter we use in Eq. (8) the steplike mask with  $\omega_{\text{high}}$ , which is much higher than the cutoff frequency. The results obtained using  $\omega_{\text{low}}$  well below and well above the resonance are shown in Fig. 4. Again, in the latter case this number is chosen to minimize the duration of the attosecond pulse. In spite of this optimization, we can see that the attopulse using off-resonant harmonics is longer and more than an order of magnitude weaker than the resonant one. Note that the parameters of the attosecond pulse formed by the resonant harmonics are not very sensitive to  $\omega_{\text{low}}$  as long as it is well below resonance; this is natural because the off-resonant harmonics are much weaker than the resonant ones. This means that practically there is much freedom in choosing such a filter as long as it transmits the resonant harmonics. Moreover, if the absorption edge of the filter is far from the resonance, the filter dispersion (which is usually pronounced only in the vicinity of the absorption edge) would not affect the attosecond-pulse duration. So, the duration of 165 as found in our calculations is close to the one which can be experimentally obtained using harmonics enhanced by giant resonance in Xe.

#### IV. ATTOSECOND PULSES GENERATION BY TWO-COLOR FIELD

Making similar calculations for the HHG by the two-color field with the parameters  $\alpha$  and  $\phi$  considered above, we find that the attopulse formed by above-resonant XUV is longer, and the one formed by below-resonant XUV is shorter than in the single-color field. This is the result of the attochirp behavior shown in Fig. 2: The absolute value of the total attochirp above the resonance is higher in the two-color case, and below the resonance the relation is reversed. Note that this leads to smaller dephasing between the harmonics near the very center of the resonance. Since these harmonics are the most intense ones, this results in an even shorter attosecond pulse than in the single-color field. Namely, the attosecond pulses formed by all XUV with a frequency higher than  $\omega_{\text{low}} = 60$  eV can be as short as 105 fs in the two-color case.

As it was shown both theoretically [15] and experimentally [29,30], the harmonic yield rapidly decreases with a decrease of the driving wavelength. So, the perspective of the generation efficiency increase using a two-color field [31–33] is especially important for the middle-infrared drivers considered here. To achieve a maximum resonant harmonic intensity in the two-color field we chose the parameters  $\alpha$  and  $\phi$  of the latter so that the resonant frequency coincides with the causticlike feature [7,34] in the dependence of the returning electron energy on the return time. Due to this feature almost all detached electrons return back with the energy close to the one of the quasistable state. This leads to a further increase of the resonant harmonic generation efficiency. Figure 5 shows the results calculated for the fundamental intensity  $2.2 \times 10^{14}$  W/cm<sup>2</sup>,  $\alpha = \frac{1}{3}$ ,  $\phi = 1.0$  (here we take into account all the electronic trajectories in the TDSE). We compare the HHG efficiency in the two-color field with that in the single-color field having an intensity equal to the sum of the intensities of the fundamental and

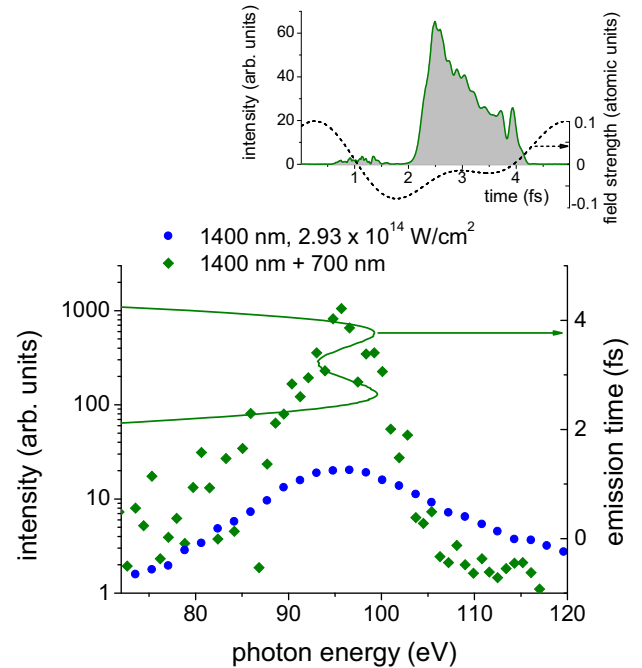


FIG. 5. Harmonic intensities generated in single-color (blue circles) and two-color (green diamonds) fields (see text for more details), and the classical return time for the two-color case. The inset shows the driving field strength (dotted line) and the resonant XUV pulse intensity (solid line) as functions of time.

the second harmonic in the two-color case. Figure 5 shows that the gain from using the two-color field with the proper parameters can be about two orders of magnitude. Together with the resonance-induced enhancement, this provides a level of conversion which can be interesting for using such harmonics as an efficient source of coherent XUV in the range of 100 eV. However, the inset in Fig. 5 shows that the generation efficiency increase using such a causticlike feature leads to a loss of the attosecond nature of the emitted XUV: The calculated XUV pulse is of approximately 2 fs duration. This value is close to the time interval when the classical electrons return with energy close to the resonant one.

#### V. CONCLUSIONS AND DISCUSSION

Thus in this paper we find conditions for which the free-motion-induced attochirp can be compensated by the resonantly induced attochirp, leading to phase synchronization of a group of resonant harmonics. It is shown that attopulses with a duration of 165 as can be obtained using resonantly enhanced harmonics generated in Xe. This duration is smaller than the minimal duration of the attosecond pulse formed by the off-resonant harmonics; it can be further reduced down to almost a hundred attoseconds using the two-color driver. Resonant HHG enhancement leads to an increase of the attopulse intensity by more than an order of magnitude and relaxes the requirements for XUV filtering: Only harmonics much lower than the resonance should be suppressed by the filter. Using a two-color field with specific parameters providing “caustic-induced” enhancement of the resonant harmonics provides a further (almost two-orders-of-magnitude) increase

of the XUV intensity at the cost of increasing the pulse duration to above 1 fs.

Note that giant resonances are observed also in other atoms, ions, and molecules. A detailed investigation of their applicability for attosecond-pulse production can be a natural development of the present study. However, our findings, in particular, the estimate of the laser field parameters required

for the phase synchronization of the resonant harmonics given by Eq. (7), should be applicable to other resonances as well.

#### ACKNOWLEDGEMENT

This study was funded by RSF (Grant No. 16-12-10279).

- 
- [1] P. M. Paul, E. S. Toma, P. Breger, G. Mullot, F. Auge, Ph. Balcou, H. G. Muller, and P. Agostini, *Science* **292**, 1689 (2001).
- [2] P. Tzallas, D. Charalambidis, N. A. Papadogiannis, K. Witte, and G. D. Tsakiris, *Nature (London)* **426**, 267 (2003).
- [3] Ph. Antoine, A. L'Huillier, and M. Lewenstein, *Phys. Rev. Lett.* **77**, 1234 (1996).
- [4] P. Salières *et al.*, *Science* **292**, 902 (2001).
- [5] S. Gilbertson, H. Mashiko, Ch. Li, E. Moon, and Z. Chang, *Appl. Phys. Lett.* **93**, 111105 (2008).
- [6] A. D. Shiner, B. E. Schmidt, C. Trallero-Herrero, H. J. Wörner, S. Patchkovskii, P. B. Corkum, J.-C. Kieffer, F. Légaré, and D. M. Villeneuve, *Nat. Phys.* **7**, 464 (2011).
- [7] D. Facciala, S. Pabst, B. D. Bruner, A. G. Ciriolo, S. De Silvestri, M. Devetta, M. Negro, H. Soifer, S. Stagira, N. Dudovich, and C. Vozzi, *Phys. Rev. Lett.* **117**, 093902 (2016).
- [8] J. Rothhardt, S. Hädrich, S. Demmler, M. Krebs, S. Fritzsche, J. Limpert, and A. Tünnermann, *Phys. Rev. Lett.* **112**, 233002 (2014).
- [9] R. A. Ganeev, T. Witting, C. Hutchison, V. V. Strelkov, F. Frank, M. Castillejo, I. Lopez-Quintas, Z. Abdelrahman, J. W. G. Tisch, and J. P. Marangos, *Phys. Rev. A* **88**, 033838 (2013).
- [10] S. Haessler, V. Strelkov, L. B. Elouga Bom, M. Khokhlova, O. Gobert, J.-F. Hergott, F. Lepetit, M. Perdrix, T. Ozaki, and P. Salières, *New J. Phys.* **15**, 013051 (2013).
- [11] N. Rosenthal and G. Marcus, *Phys. Rev. Lett.* **115**, 133901 (2015).
- [12] R. A. Ganeev, *J. Mod. Opt.* **59**, 409 (2012).
- [13] R. A. Ganeev, *High-Order Harmonic Generation in Laser Plasma Plumes* (Imperial College Press, London, 2012).
- [14] M. V. Frolov, N. L. Manakov, T. S. Sarantseva, M. Y. Emelin, M. Y. Ryabikin, and A. F. Starace, *Phys. Rev. Lett.* **102**, 243901 (2009).
- [15] V. Strelkov, A. Sterjantov, N. Shubin, and V. Platonenko, *J. Phys. B* **39**, 577 (2006).
- [16] V. Strelkov, *Phys. Rev. Lett.* **104**, 123901 (2010).
- [17] M. Tudorovskaya and M. Lein, *Phys. Rev. A* **84**, 013430 (2011).
- [18] V. V. Strelkov, M. A. Khokhlova, and N. Yu. Shubin, *Phys. Rev. A* **89**, 053833 (2014).
- [19] V. Kapoor, *Phys. Rev. A* **93**, 063408 (2016).
- [20] V. V. Strelkov, M. A. Khokhlova, A. A. Gonoskov, I. A. Gonoskov, and M. Yu. Ryabikin, *Phys. Rev. A* **86**, 013404 (2012).
- [21] V. V. Strelkov, *Phys. Rev. A* **74**, 013405 (2006).
- [22] Y. Mairesse *et al.*, *Science* **302**, 1540 (2003).
- [23] P. B. Corkum, *Phys. Rev. Lett.* **71**, 1994 (1993).
- [24] K. J. Schafer, B. Yang, L. F. DiMauro, and K. C. Kulander, *Phys. Rev. Lett.* **70**, 1599 (1993).
- [25] M. A. Khokhlova and V. V. Strelkov, *Phys. Rev. A* **93**, 043416 (2016).
- [26] V. T. Platonenko and V. V. Strelkov, *Quantum Electron.* **27**, 779 (1997).
- [27] R. López-Martens *et al.*, *Phys. Rev. Lett.* **94**, 033001 (2005).
- [28] E. Goulielmakis *et al.*, *Science* **320**, 1614 (2008).
- [29] P. Colosimo *et al.*, *Nat. Phys.* **4**, 386 (2008).
- [30] A. D. Shiner, C. Trallero-Herrero, N. Kajumba, H. C. Bandulet, D. Comtois, F. Legare, M. Giguere, J. C. Kieffer, P. B. Corkum, and D. M. Villeneuve, *Phys. Rev. Lett.* **103**, 073902 (2009).
- [31] H. Eichmann, A. Egbert, S. Nolte, C. Momma, B. Welleghausen, W. Becker, S. Long, and J. K. McIver, *Phys. Rev. A* **51**, R3414 (1995).
- [32] I. J. Kim, C. M. Kim, H. T. Kim, G. H. Lee, Y. S. Lee, J. Y. Park, D. J. Cho, and C. H. Nam, *Phys. Rev. Lett.* **94**, 243901 (2005).
- [33] A. S. Emelina, M. Yu. Emelin, R. A. Ganeev, M. Suzuki, H. Kuroda, and V. V. Strelkov, *Opt. Express* **24**, 13971 (2016).
- [34] O. Raz, O. Pedatzur, B. D. Bruner, and N. Dudovich, *Nat. Photonics* **6**, 170 (2012).